Spatial and Temporal Evolution of Urban Patterns in the China Greater Bay Area Based on Remote Sensing of Nighttime Lights

Linyuheng Hu[1, *, †], Xinzhi Pan[2, a, †]

[1]Wuxi University Wuxi, China

[2]Anhui Nomal University Wuhu, China

* Corresponding Author Email: 20192367006@stu.cwxu.edu.cn, [a]xinzhipan@ahnu.edu.cn

†These authors contributed equally.

Abstract. With the advancement of urbanization in China, the rapid expansion of cities has reduced the alternative land use and intensified the conflict between people and land, and the adaptation and optimization of urban spatial patterns have become an important work in current urban research. Based on the comprehensive modified the long-term series DMSP-OLS and NPP-VIIRS nighttime lighting data, the spatial analysis method of GIS and urban expansion indicators are used to reveal the spatial and temporal change process of urban built-up areas in the center of gravity of Guangdong-Hong Kong-Macao Greater Bay Area from 1992 to 2020. The results reveal that the built-up area of the urban agglomerations in the study area generally shows an increasing trend year by year, but there are some periods when the area decreases or remains unchanged, while the expansion rate shows a gradual decrease over a long time scale. The compactness of the urban agglomerations in the GBA decreases over time, and the fractal dimension fluctuates but remains unchanged, while the spatial distribution of the urban agglomerations in the GBA shows a "southwest-northeast" direction during 1992-2020, with the center of gravity moving to the northeast gradually. On the side, the urban expansion shows a fluctuation of "diffusion-coalescence-diffusion". The expansion of urban built-up areas is influenced by both natural and socio-economic factors, and the degree of influence varies in different periods.

Keywords: Night light remote sensing; DMSP-OLS; NPP-VIIRS; built-up area; The China Greater Bay Area.

1. Introduction

City clusters are now the most prevalent type of new urbanization and an essential platform for promoting coordinated regional development and participating in international competition and cooperation. Metropolitan areas consist of areas of urbanization within an agglomeration related to a megacity or a large city, with a strong radiation-driven function, with a commuting radius of one hour as their primary scope [1]. A key component of the 14th Five-Year Plan is the "development and growth of urbanized areas and clusters", which is expected to create a "new windfall for economic growth" and the "largest structural potential for Chinese development in the next five to ten years". "Building the Guangdong-Hong Kong-Macao Greater Bay Area (the GBA) and a supreme urban agglomeration", "Increasing exchanges and cooperation between Mainland area, Hong Kong, and Macau", was the central directive of the Greater Bay Area Development Planning Outline" issued in February 2019. There are still disparities in development within the Greater Bay Area, and the alignment and inclusivity of the region need to be further strengthened. Some regions and fields are still experiencing homogenous competition and resource mismatches. Hong Kong's economic growth is lacklustre, Macau's economic structure is relatively simple and it lacks the resources to further develop its economy, and the market economy system of the PRD city cluster needs to be optimized and improved. Currently, the area is experiencing bottleneck restrictions, tighter resource, and energy limits, intensifying ecological environment pressure, and diminishing demographic dividends.

Recent advancements in urban remote sensing and geographic information systems have enabled monitoring of urban development patterns at multiple spatial scales, particularly in remote sensing images of lights at night, allowing for more efficient and accurate research processes. Night light remote sensing is a relatively new type of remote sensing technology that has recently gained an amount of attention. At night, satellites can detect visible light from sources, such as street lights, fishing boats, and fire spots when the sky is clear. Under these conditions, visible light is to create an image of the earth. In contrast to daytime remote sensing, nighttime remote sensing may depict human social events; as a result, it has been widely used for data mining methods in socioeconomic applications. Traditional spatial and temporal pattern monitoring of urban agglomerations relies primarily on statistical yearbook data. Although the statistical yearbook is rich in data, it cannot effectively reflect the accurate spatial distribution of urban built-up areas. With advantages of intuitiveness, objectivity, timeliness, and economy, remote sensing technology has been widely used in monitoring the dynamic changes of urban spatial and temporal patterns [2]. In contrast to the traditional economic model and single data source, this paper integrates DMSP/OLS and NPP/VIIRS night-light remote sensing image data for consistency correction. By establishing a series of stable night-light remote sensing datasets, the Spatio-temporal pattern of urban agglomerations in the GBA is monitored to expose the Spatio-temporal evolution characteristics of the scale structure of urban agglomerations in the region in the past 10 years. This study aims to provide a reference for the management and planning of this urban agglomeration, as well as for the synergistic development of urban agglomerations, and even a methodological reference for the study of the evolution of the Spatio-temporal pattern of other urban agglomerations.

2. Data and methods

2.1. Overview of the study area

Guangzhou - Hong Kong - Macao Greater Bay Area, also called the Greater Bay Area (GBA), comprises 12 cities and encompasses 56,000 km^2, which is one of the most open and economically vibrant areas of strategic significance in the national economic growth.

The Greater Bay Area is situated in the south-east of China with the characteristic of subtropic monsoon: high-temperature summer more rain, winters, and mild less rain raining and hot during the same period. The geometric center here is located at the junction of Guangzhou and Foshan, where there is a county called Nansha County (113°36’ 12’’ E, 22°40’28’’ N). We have an average of 1,300 to 2,500 millimeters a year of rain and the annual mean temperature is 22.5 degrees. In 2020, the Greater Bay Area’s total population has reached more than seventy million. Meanwhile, its gross regional production is 1.15 billion. The built-up area of the Greater Bay IS about 56,000 square kilometers (Fig.1).

The Greater Bay Area is being developed not only as a vivid world-class urban agglomeration, a global base for scientific and technological innovation, a tower of strength for the Belt and Road Initiative, and a classic demonstration location for in-depth collaboration and communication between the mainland, Hong Kong, and Macao, as well as a high-quality living circle suited for living, working, and touring, and a prototype zone for high-quality development. Figure 1 is a diagram of the administrative regions of the GBA.

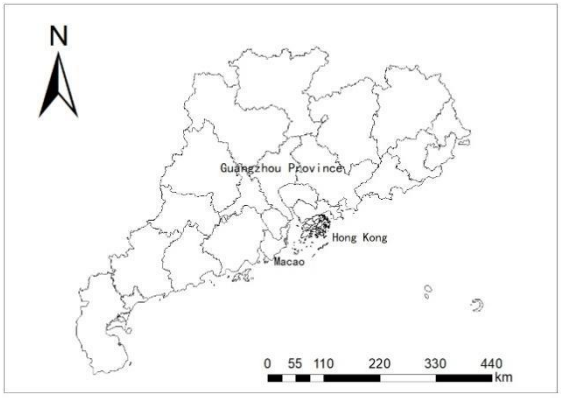

Fig 1. Map of the GBA

2.2. Data Sources

The night-light data that we used in this study are NPP/VIIRS data and DMSP/OLS data. The local policy information and the statistic yearbooks.

The DMSP/OLS data is provided by the Earth Observation Organization (http://ngdc.noaa.gov/eog/). The data were collected by OLS sensors on six different DMSP satellites from 1992 to 2012. After removing the influence of fire and explosion, the data were synthesized annually. The data pixel values range is from 0 to 63, spatial resolution is 1 km (original resolution of DMSP/OLS sensor is 2.8 km, production resampled is 1 km). The data coverage is 180°W-- 180°E, 65°s--75°N.

Our NPP/VIIRS data is provided by Earth Observation Group (http:// eogdata.mines.edu/products/vnl/). In the part of Monthly Cloud-free DNB Composite, we can download the version 1 monthly serious NPP/VIIRS data of China from 2012 to 2020. Globally, the version 1 monthly serious is executed utilizing two distinct settings. The first one, labeled "vcm," excludes data affected by stray light. The second one, labeled "vcmsl," has these values if the radiance measurements have been corrected for stray light. The image resolution is 15 arc-second (about 500 meters at the Equator), CRS is EPSG:4326 (geographic latitude/longitude), and the coverage is 180°W-- 180°E, 65°s--75°N [1].

The administrative planning boundary that we used is the 1:1,000,000 administrative planning boundary of Prefecture-level cities in China. The built-up area information in the GBA comes from the Statistical Yearbook of Chinese cities and the local policy information is from the official website of the Central People's Government of the Republic of China.[2]

2.3. Research methods

In this study, we carried out mutual correction and continuity correction for DMSP/OLS data and NPP/VIIRS data respectively, and then supersaturation correction and consistency correction were carried out for the two data to establish night-light remote sensing data of long time series from 1992 to 2020. Using a reference-based method, the spatial distribution of built-up areas was extracted and studies every five years. Based on it, the standard deviation ellipse was calculated to study the evolution of urban patterns in the Greater Bay Area.

2.4. Calibration of DMSP/OLS data

This paper presents a stable light image classification based on an invariant target region. The classification method consists of three steps: 1. Saturated pixel and unsaturated pixel classification. 2. Saturation correction and mutual calibration of saturated pixels. 3. Mutual calibration of unsaturated pixels.

Classification of saturated and unsaturated pixels for stable light images

In the stable light image, when the DN value is greater than 50, especially when it is above 55, the pixel number begins to rise rapidly, which is contrary to the overall downward trend. As a result,

when the pixel DN value is greater than 55, the stable light image pixel is severely saturated. In this study, we selected the pixel DN value that is equal to 55 as the threshold value to distinguish saturated and unsaturated pixels from stable light images [3].

Saturation correction and mutual calibration of saturated pixels.

Saturated pixel in the stable light image's aturation correction equation:

$$DN_c = d \times DN_{RC}^{e}$$

In this formula(1),[4] DN_c value symbolizes the stabilized light image's pixel DN value that after correction; DN_{RC} value symbolizes the pixel DN value of the radiation-calibrated light image as the reference image. And *d* and *e* are different regression parameters.

Due to the lack of comparability between radiation-calibrated images, saturated pixels of the stable light image after saturation correction still cannot be compared with each other, which requires further mutual calibration of the saturated pixels after saturation correction.

$$DN_{ICSC} = C_1 \times DN_{RC} + C_0$$

In this formula(2) [4], DN_{ICSC} value symbolizes the pixels DN value of the radiometric light image after mutual correction; DN_{RC} value symbolizes the pixels DN value of the radiation-calibrated light image; C_1 and C_0 are model parameters.

Mutual correction of unsaturated pixels

$$DN_c = a \times DN^2 + b \times DN + c$$

In this formula(3) [4], *DN* value symbolizes the stable light image's pixel DN value which is going to be corrected; DN_C value symbolizes the stable light image's pixel DN value after correction; *a, b, and c* are different regression parameters. In order to ensure that the region without light value (DN = 0) in the stable light image remains consistent after correction, the pixel with DN value equal t 0 is not put into this formula.

Finally, the saturated and unsaturated pixels of the original sable light images were replaced by the saturated pixels after saturation correction and mutual calibration, and unsaturated pixels after mutual calibration respectively. And then the stable light image after classification correction was obtained.

2.5. Calibration of NPP/VIIRS data

Calibration of NPP/ VIIRS data is divided into three parts: NPP/VIIRS data re-projection and resampling, data outliers alignment, and data correction between years.

NPP/VIIRS data re-projection and resampling: convert the projection coordinates of NPP/VIIRS original data to Krasovsky_1940_Albers projection and resampled to 1000 meters to keep consistent with DMSP/OLS data, and cut the image to obtain the image data of the study area.

Data outliers alignment: NPP/VIIRS data are sensitive to the brightness of lights, which includes other types of lights, for example, fires, gas flares, and volcanoes, requiring processing of outliers. The process consists of two parts. The first is the maximum light value processing. The maximum light brightness in the region is taken as the maximum threshold. If the light the pixel's value in the whole image is greater than the maximum threshold, the pixel will be assigned as the maximum threshold. The second is noise processing [5].

Data correction between years: Inter-annual calibration of NPP/VIIRS data has the same principle as DMSP/OLS data. The data from 2013 to 2020 after outlier processing were corrected and formed continuous NPP/VIIRS data [6].

2.6. Mutual correction between DMSP/OLS data and NPP/VIIRS data

In the pre-processing of DMSP/OLS data and NPP/VIIRS data, there is continuity and comparability in a single data after gradual correction. In order to have continuity and comparability of the two types of night-light data, they need to be adjusted to the same ruler: Calibrate the DN

values of DMSP/OLS data to the luminance range scale of NPP/VIIRS data, or calibrate the DN values of NPP/VIIRS data to the luminance range scale of NPP/VIIRS. Finally, all the data were on the same scale and can be directly compared later to gain long-term image data from 1992 to 2020.

Mutual correction: In mutual calibration, the most important thing is to establish the DMSP/OLS data and NPP/VIIRS data's regression model of DMSP/OLS data and NPP/VIIRS data in 2012 or 2013 that after pre-processing in the study area and generating the fitting function. DMSP/OLS data were used to correct the NPP/VIIRS data, and the brightness values of the two lights were corrected to the same scale range. Finally, the regression model with a high correlation in the fitting results was selected:

$$Y = a\,ln(X) + b$$

In this formula(4), X symbolizes the DN value of NPP/VIIRS before calibration; Y symbolizes the DN value converted from NPP/OLS data to DMSP scale after correction; a and b are both the logarithmic regression model's correction parameters .

Intra-year fusion and inter-year correction: Annual fusion operation was performed for the two types of night-light data in 2013, as well as the inter-annual correction was performed for all the data in 2013. The correction operation is similar to that of DMSP/OLS data.

2.7. Extraction of built-up area and evaluation of the accuracy

Comparing several methods, we settled on the reference-based method. The reference-based method is one kind of threshold method. It is very scientific and can produce high-precision results in a simple way.

This method is to set a series of lighting thresholds and compare the built-up area given by these lighting thresholds with the data published in the government statistics. Then take the threshold which has the smallest error as the best choice.

Our built-up area data of each city in The Great Bay from 1992 to 2020 is obtained from the Statistical Yearbook of Chinese cities. Import one-year data into an Excel table, and enter the formula (= F_AREA/1000000) to get the threshold. According to the definition of the urban area, we use statistical yearbook built-up area data to calculate the relative and absolute error and measure the accuracy and results.

2.8. Standard deviation ellipse

To analyze the point of built-up area, we used the standard deviation ellipse. It was first proposed by D. Welty Lefever [7], who is a sociology professor of the University of Southern California, in 1926. As a result, it is also called Lefever's "Standard Deviation Ellipse".

We can use the standard deviation ellipse to analyze and calculate the direction and distribution of a point simultaneously. Its greatest advantage is that as long as we measure the direction and distribution of a set of data, an ellipse will appear.

According to the fitting standard deviation ellipse, we can extract the center of the ellipse to represent the core of urban agglomeration and get the ellipse's major and minor axes to represent the main distribution and scope of urban agglomeration respectively [8].

The formula for determining an ellipse's center is as follows:

$$SDEx = \sqrt{\frac{\sum_{i=1}^{n}(x_i-\bar{X})^2}{n}}$$

$$SDEy = \sqrt{\frac{\sum_{i=1}^{n}(y_i-\bar{Y})^2}{n}}$$

In (5) and (6), $\bar{X}$ and $\bar{Y}$ is the coordinates of the ellipse's core. x_i and y_i are the coordinates of pixel NO. i and n are the total number of pixels.

The formula for determining the direction of the ellipse is as follows. Based on the X-axis, assume that due north is 0 degrees and rotate clockwise:

$$\tan\theta = \frac{A+B}{C}$$

$$A = (\sum_{i=1}^{n} \tilde{x}_i^2 \quad \sum_{i=1}^{n} \tilde{y}_i^2$$

$$B = \sqrt{(\sum_{i=1}^{n} \tilde{x}_i^2 - \sum_{i=1}^{n} \tilde{y}_i^2)^2 + 4(\sum_{i=1}^{n} \tilde{x}_i \tilde{y}_i)^2}$$

$$C = 2\sum_{i=1}^{n} \tilde{x}_i \tilde{y}_i$$

In the formulas above, θ symbolizes the direction angle of an ellipse, which is the angle between the X-axis and due north. x_i and y_i are the coordinates of pixel NO. i.

The formula for determining the lengths of the X-axis and Y-axis is as follows:

$$\sigma_x = \sqrt{2}\sqrt{\frac{\sum_{i=1}^{n}(\tilde{x}_i \cos\theta - \tilde{y}_i \sin\theta)^2}{n}}$$

$$\sigma_y = \sqrt{2}\sqrt{\frac{\sum_{i=1}^{n}(\tilde{x}_i \sin\theta + \tilde{y}_i \cos\theta)^2}{n}}$$

In (11) and (12), σ_x and σ_y are the standard deviations of the X-axis and Y-axis of the ellipse, which are the lengths of the X-axis and Y-axis. θ represent the direction angle of an ellipse, and n is the total number of pixels.

3. Analysis of data results

3.1. Calibration of NPP/VIIRS data and DMSP/OLS data analysis

Before the continuity correction, there were obvious inconsistencies between the TDN and TLP of OLS images from different DMSP satellites and different years of the same satellite. After the correction, the TDN and TLP continuity of OLS data from different DMSP satellites were significantly improved, showing a trend of stable increase year by year, and there were no more disorderly fluctuations and repeated phenomena, indicating that the continuity correction improved the continuity and stability of DMSP/OLS data.

The border between urban and rural regions in the photos is blurry as a result of the poor spatial resolution of the DMSP/OLS images as well as the difficulties of image brightness saturation and light spillover, and the brightness of the image elements in the urban core area to the rural area changes slowly, while the contrast between the built-up area and the non-built-up area around the built-up area in the NPP/VIIRS images is much more obvious, and the change of the urban image elements to the suburban image elements is very significant.

From the comparison in the figure , it can be found that the logarithmic transformation can well suppress the sudden change of the brightness of the urban image elements to the suburban image elements in the NPP/VIIRS image, and make the transition from the brightness of the urban image elements to the brightness of the suburban image elements become more smooth so that the consistency of the NPP/VIIRS and DMSP/OLS data can be improved [9]. Figure 2 shows a comparison of the images obtained from different sensors before and after correction.

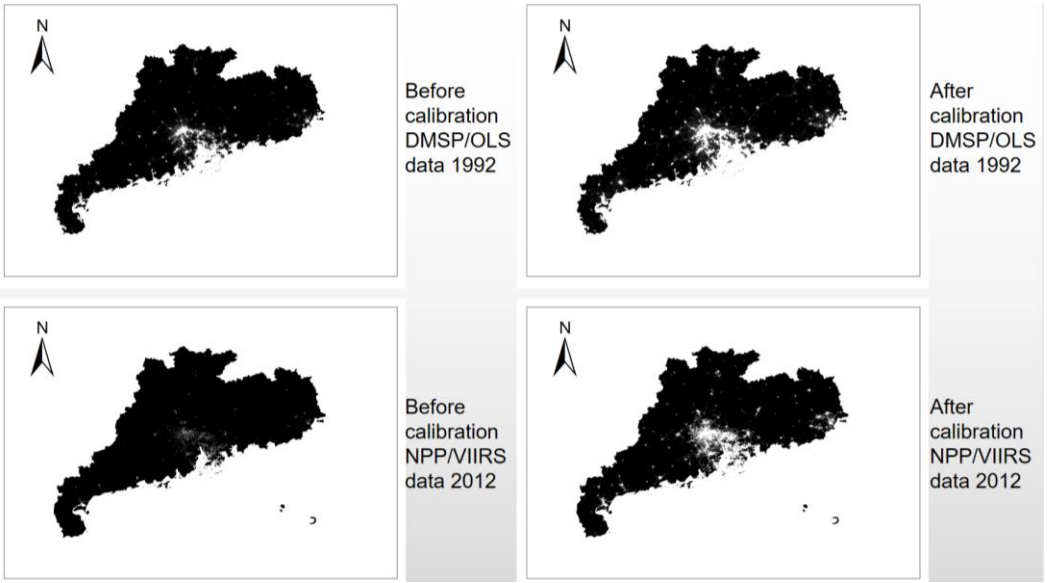

Fig 2. Comparison of DMSP/OLS images in the GBA over the year 1992 before and after transformation and comparison of NPP/VIIRS images in the GBA over the year 2012 before and after transformation.

3.2. Threshold extraction analysis

By combining the built-up area in the statistical yearbook, the built-up area threshold is obtained through the reference comparison method, and the built-up area range of the GBA in different years is obtained through the threshold extraction. between 1992 and 2020, the built-up area of the core area of the Greater Bay Area shows rapid growth, with the built-up area growing from 1843.51 km2 in 1992 to 6621.15 km2 in 2020, an increase of 259.15%. The built-up area's average annual growth rate reached 9.2% in 28 years, but the growth rate has been slowing down.

Among them, the built-up areas of Guangzhou-Foshan and Hong Kong-Shenzhen core areas are expanding more obviously, but there are still large differences within the core areas. In the Guangzhou-Foshan core area, the outspread of the built-up area of Guangzhou is dominant, and the outspread of the built-up area of Foshan is less, but the border area of the two cities is gradually incorporated into the scope of the built-up area of the two cities, and the expansion of the built-up area promotes the construction of infrastructure, accelerates the development of Guangzhou-Foshan co-city, and also strengthens the position of Guangzhou as a central city. In the Hong Kong-Shenzhen core area, the expansion of Shenzhen's built-up area dominates, but as the built-up areas of the two cities slowly border each other, the connection between the two cities is also deepening. While the outspread of the built-up area in the Macau-Zhuhai's core is relatively slow, Zhuhai dominates it and Macau is difficult to expand on a large scale due to its geographical location. However, the expansion of Zhuhai's built-up area is mainly bordered by Macau's built-up area, so the connection between the two areas is gradually increasing. Dongguan, as a node city connecting the two cores of Guangzhou-Foshan and Hong Kong-Shenzhen, has a more obvious expansion of its built-up area, and the scale of expansion is comparable to that of Shenzhen. The built-up area of Dongguan is also gradually connected to Shenzhen and Guangzhou, bridging the two core areas and deepening the connection between cities on the east coast. Zhongshan, the node city on the west bank, is relatively slow in expanding its built-up area, comparable to Foshan and Zhuhai, and the built-up area is relatively independent, not bordering Foshan and Zhuhai, so the role of the node city is relatively limited. From the perspective of the east and west coasts, it is obvious that the expansion of the built-up area on the east coast is more obvious, while the development of the built-up area on the west coast is slower, and the difference between the east and west coasts is increasing [10].

3.3. Standard deviation elliptic analysis

Figure 3 presents the spatial and temporal trends and weighted standard deviation ellipses of the center of gravity of the urban agglomeration in the Greater Bay Area in 1992, 1995, 2000, 2005, 2010, 2015, and 2020 based on the fitted nighttime light data set after processing. Based on the weighted standard deviation ellipses, the spatial evolution trends of this urban agglomeration are analyzed, including the changes in the center of gravity and the main distribution direction.

The center of gravity of the urban agglomeration in the Greater Bay Area from 1992 to 2020 is relatively stable, always located near the administrative boundary of Guangzhou and Dongguan cities. The center of gravity generally tends to move in the northeast direction, and in the course of the five shifts of the center of gravity, it moves to the northwest once, to the northeast four times, and once without significant changes.

During the period 1992 to 2020, the center of gravity of the built-up area moves mainly from the south to the northwest, from the position of 113°762 E and 22°762 N in 1992 to the position of 113°685 E and 22°844 N in 2020 (Figure 4). from 1992 to 1998, the center of gravity of the urban built-up area outspread in the core area of the GBA was located at the mouth of the Pearl River; while After 1998, the center of gravity of urban built-up area outspread shifted to Humen Town, Dongguan City, and has kept moving to the northeast since then, but has not left Humen Town.

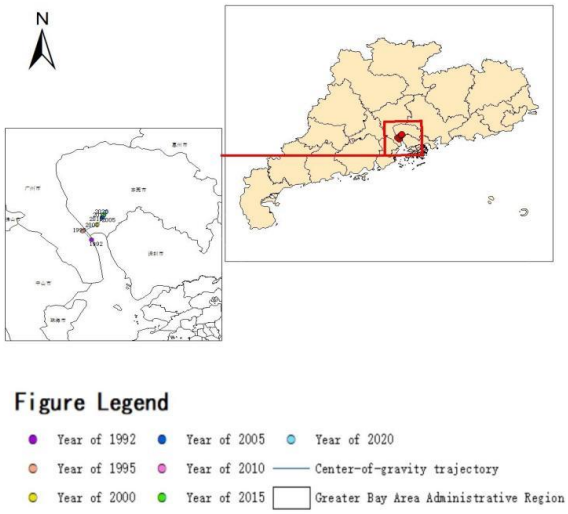

(a) center-of-gravity trajectory

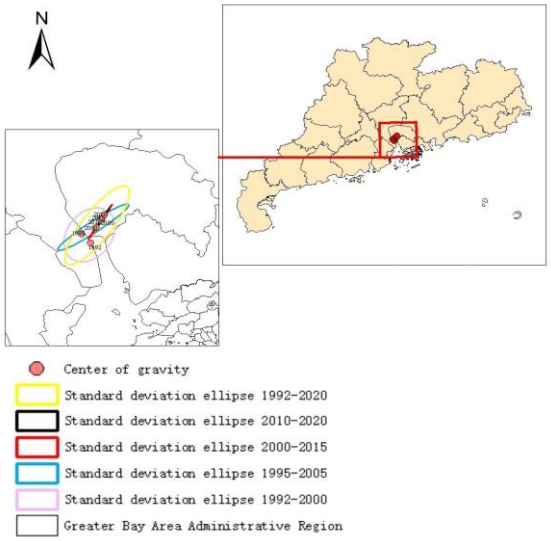

(b) Standard deviation elliptic of different periods

Fig 3. The consequence of the weighted standard deviation ellipse calculation, built-up area extraction, and shift of the center of gravity of the Greater Bay Area.

From 1992 to 2020, the center of gravity shifted 20.67 km to the north, moving 1.09 km to the north each year on average, among which the shifting speed was rapid between 1992 and 2003, moving to the northeast with a speed of 3.29 km-a-1, but in Between 2003 and 2020, the movement speed decreases, moving northeastward with a speed of 0.30 km-a-1. Although the center of gravity of urban built-up areas in the centre of gravity of the Greater Bay Area gradually shifts to the northeast, the center of gravity is always located in the south-central part of the study area, and the growth of built-up areas in its core cities (e.g., Guangzhou and Shenzhen) is much higher than that in other regions [10].

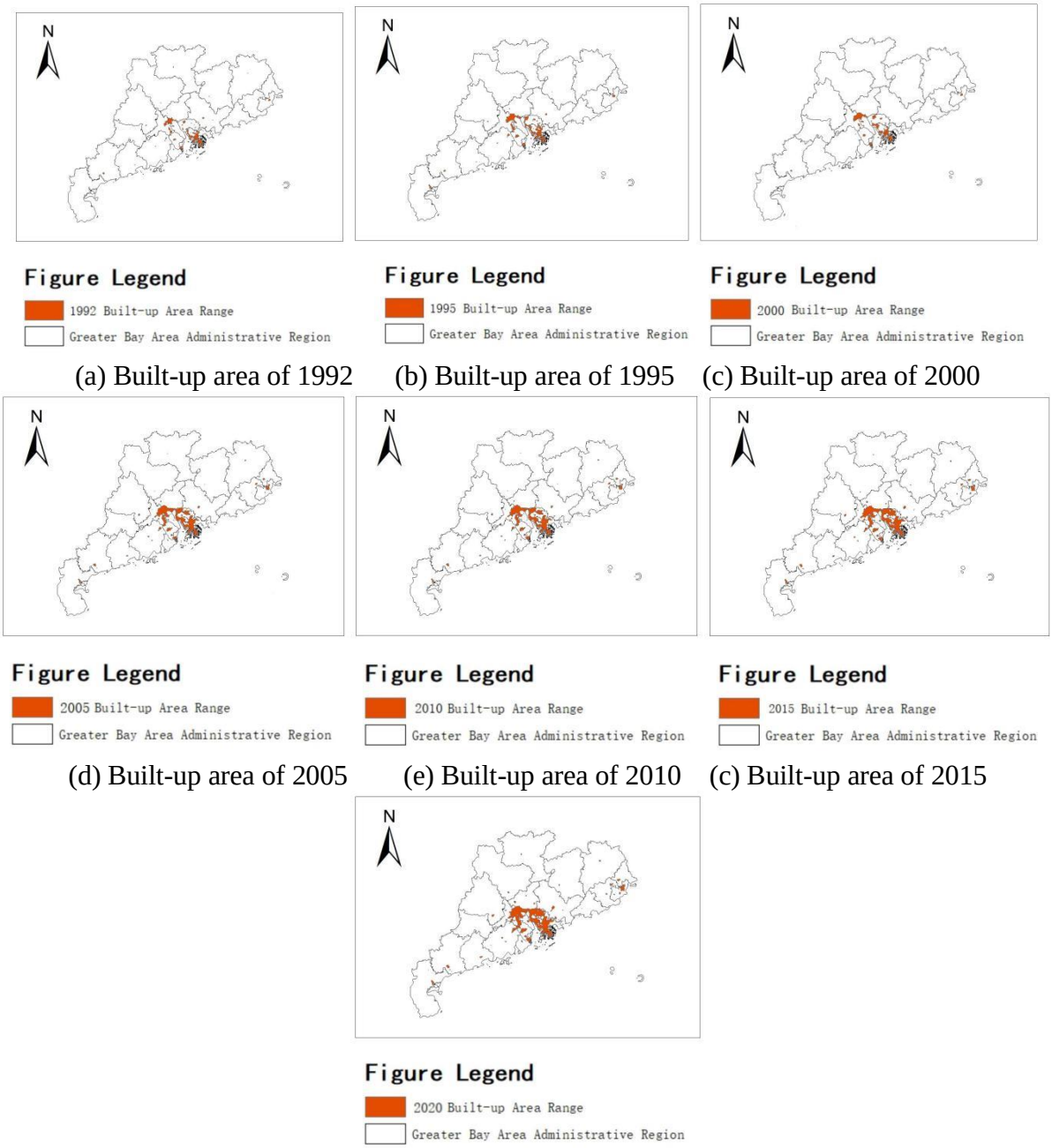

(a) Built-up area of 1992 (b) Built-up area of 1995 (c) Built-up area of 2000

(d) Built-up area of 2005 (e) Built-up area of 2010 (c) Built-up area of 2015

(g) Built-up area of 2020

Fig 4. Evolution of built-up area in the Greater Bay Area from 1992 to 2020

4. Conclusion

As one of the regions with the best urbanization foundation in China, the urban development process and spatio-temporal characteristics of urbanization in the GBA region are of great

significance to the national urban development and pattern. In order to properly monitor the geographical and temporal features of cities, this research examines the NPP/VIIRS and DMSP/OLS night-light remote sensing data for the integrated region of the GBA. The changes of the built-up area of the GBA from 1992 to 2020 are obtained by comparing the two scales of space and time, so as to get the urban construction situation and the change of the urban center of gravity.

The center of gravity of the Greater Bay Area cities is relatively stable according to the light-weighted standard deviation ellipse calculation. Its center of gravity has always been located near Humen Town, Dongguan, with small inter-annual variation and no obvious trend of change. There is no obvious change in the direction angle of the ellipse and the direction angle of the ellipse presents a southwest-northeast distribution. The flattening of the ellipse change significantly in 2000, indicating that the centripetal force and direction of urban agglomeration development changed significantly in this year. In addition, POI data, GDP data, and population grid data can also be imported into future research to verify correlation and analyze economic development from multiple perspectives through data visualization.

References

[1] Levin N, Kyba C C M, Zhang Q L, et al. Remote sensing of night lights: a review and an outlook for future. Remote Sensing of Environment, 2020, 237(1):111443.

[2] Ball S, Petsimeris P. "Mapping urban social divisions." Forum Qualitative Sozialforschung/Forum: Qualitative Social Research.. 2010, 11(2), pp. 16-27.

[3] Wang Z, Yao F, Li W F, et al. Saturation correction for nighttime lights data based on the relative NDVI. Remote Sensing, 2017, 9:759.

[4] Cao Z Y, Wu Z F, Mi S J, et al. A method for classified correction of stable DMSP/OLS nighttime light imagery across China. Journal of Geo-information Science, 2020, 22(2), pp.246-257.

[5] Shi K, Yu B, Huang Y, et al, Evaluating the ability of NPP/VIIRS nighttime light data to estimate the gross domestic product and the electric power consumption of China at multiple scales: a comparison

[6] Zhang B R, Li J, Wang M G, Daun P, et al. Mutual correction of DMSP/OLS in Mainland China. Remote Sensing. 2021. 147.3, pp.446-457.

[7] Lefever D W. Measuring geographic concentration by means of the standard deviational ellipse. American Journal of Sociology, 2016, 32(1), pp.88-94.

[8] Vartholomaios, A. A geospatial analysis of the influence of landscape and climate on the location of Greek vernacular settlements using GIS. Applied Geomatics, 2019, 11(2), pp.197-213.

[9] Xu Z S, Xu Y M. Study on the spatio-temporal evolution of the Yangtze River Delta urban agglomeration by integrating Dmsp/Ols and Npp/Viirs nighttime light data. Journal of Geo- information Science, 2021, 23(5), pp.837- 849.

[10] Lu Y., Yu Y., Liu G.. Spatial and Temporal Dynamics of Urban Build-up Area in the Core Ara of Guangdong-Hong Kong-Macao Greater Bay Area Based on Nighttime Lighting Data During 1998—2017. Journal of Ecology and Rural Environment, 2021, 37(9) pp.1147-1157.